



OPEN

Somatostatin-expressing interneurons modulate neocortical network through GABA_B receptors in a synapse-specific manner

Dominik Kanigowski¹, Karolina Bogaj¹, Alison L. Barth² & Joanna Urban-Ciecko^{1,2}✉

The firing activity of somatostatin-expressing inhibitory neurons (SST-INs) can suppress network activity via both GABA_A and GABA_B receptors (Rs). Although SST-INs do not receive GABA_AR input from other SST-INs, it is possible that SST-IN-released GABA could suppress the activity of SST-INs themselves via GABA_BRs, providing a negative feedback loop. Here we characterized the influence of GABA_BR modulation on SST-IN activity in layer 2/3 of the somatosensory cortex in mice. We compared this to the effects of GABA_BR activation on parvalbumin-expressing interneurons (PV-INs). Using *in vitro* whole-cell patch clamp recordings, pharmacological and optogenetic manipulations, we found that the firing activity of SST-INs suppresses excitatory drive to themselves via presynaptic GABA_BRs. Postsynaptic GABA_BRs did not influence SST-IN spontaneous activity or intrinsic excitability. Although GABA_BRs at pre- and postsynaptic inputs to PV-INs are modestly activated during cortical network activity *in vitro*, the spontaneous firing of SST-INs was not the source of GABA driving this GABA_BR activation. Thus, SST-IN firing regulates excitatory synaptic strength through presynaptic GABA_BRs at connections between pyramidal neurons (Pyr-Pyr) and synapses between pyramidal neurons and SST-INs (Pyr-SST), but not Pyr-PV and PV-Pyr synapses. Our study indicates that two main types of neocortical inhibitory interneurons are differentially modulated by SST-IN-mediated GABA release.

The compound functions of the neocortex depend on neuronal microcircuits of highly interconnected glutamatergic (excitatory) neurons and GABAergic (inhibitory) interneurons. The GABA_B receptors (GABA_BRs) are G-coupled metabotropic receptors that are expressed pre- and postsynaptically, where they inhibit neuronal activity via the modulation of the calcium and potassium channels, respectively. GABA_BRs can be found on both excitatory and inhibitory cells, however, the distribution and function of GABA_BRs on specific neuronal populations and their inputs and outputs are not well-characterized, especially for molecularly and anatomically diverse inhibitory neuron subtypes that have critical roles in shaping network output. Among these interneurons, somatostatin-expressing and parvalbumin-expressing interneurons (SST-INs and PV-INs, respectively) comprise more than half of the inhibitory interneurons in the mouse neocortex^{1,2}. It has been believed that PV-INs target mainly soma, proximal parts of dendrites or the axon initial segment³, whereas SST-INs are considered to innervate primarily (but not exclusively) distal parts of pyramidal (Pyr) neurons⁴. Interneurons show high basal firing activity that can be regulated by brain state, behavioral tasks, and also during learning⁵⁻⁷. The activity of neocortical PV- and SST-INs is regulated in a characteristic and often opposing manner⁸. For example, in the mouse barrel cortex, L2/3 SST-INs are spontaneously active during quiet wakefulness, whereas their activity is reduced during both passive and active whisker movements^{8,9}. In contrast, PV-INs fire spontaneously during the quiet wakeful state and are profoundly activated by whisker sensing⁸. How brain state regulates the activity of these two interneurons is the subject of intense investigations.

SST-INs both directly and indirectly control neocortical network activity. Prior studies indicate that *in vivo* optogenetic silencing of SST-IN firing paradoxically increases the activity of neighboring Pyr neurons⁸. Our previous *in vitro* study identified a synaptic mechanism that may underlie this phenomenon, showing that SST-IN spontaneous activity strongly silences excitatory synaptic transmission between L2/3 Pyr neurons in mouse somatosensory cortex¹⁰. The effect is mediated by the presynaptic GABA_BR activation, which reduces

¹Laboratory of Electrophysiology, Nencki Institute of Experimental Biology, Warsaw 02-093, Poland. ²Department of Biological Sciences and Center for the Neural Basis of Cognition, Carnegie Mellon University, Pittsburgh, PA 15213, USA. ✉email: j.ciecko@nencki.edu.pl

neurotransmitter release probability^{11–13}. These data indicate that spontaneous activity of SST cells provides tonic inhibition to Pyr neurons, decoupling them from the network during quiet states.

SST-IN spontaneous firing may control synaptic transmission in a global- or synapse-specific manner through GABA_ARs. It has been identified that GABA_ARs can act as autoreceptors and suppress GABA release¹⁴. Most GABAergic terminals have been found to possess GABA_ARs, however, little is known of GABA_AR modulation in specific interneuron subtypes. Here, we compared the effects of GABA_ARs on spontaneous firing, intrinsic excitability and excitatory synaptic inputs and inhibitory outputs of SST- and PV-INs in L2/3 of mouse somatosensory cortex. We also investigated how the spontaneous firing of SST-INs modulates synaptic transmission input from Pyr neurons onto these interneurons. Using in vitro electrophysiology, pharmacological and optogenetic tools, we found that SST-INs modulate neocortical network through the tonic activation of the GABA_ARs in a highly synapse-specific manner.

Results

SST-IN spontaneous network activity is immune to tonic modulation through GABA_ARs. SST-INs can be spontaneously active without excitatory synaptic input¹⁵. This spontaneous firing is linked to high levels of GABA released from SST-IN terminals and can influence GABA_ARs across local networks. Here we asked whether the spontaneous activity of SST-INs might control their own activity via a feedback mechanism mediated by GABA_ARs. To analyze how GABA_ARs modulate activity of SST-INs we recorded their spontaneous firing in vitro using mACSF which has been known to mimic natural cerebrospinal fluid¹⁶ and evokes a high level of network activity^{10,17,18}. Modified ACSF enabled us to analyze neuronal function in the condition of the background slow oscillatory activity that mimics the quiet state in vivo¹⁹. In this condition, L2/3 SST-INs showed elevated spontaneous firing, ranging from 0 to 9 Hz (Fig. 1) consistent with other studies^{8,20}. Bath application of the GABA_AR agonist baclofen reduced the spontaneous firing of SST-INs by 60% from 2.16 ± 2.71 Hz in control to 0.88 ± 1.17 Hz in baclofen (Fig. 1A,B; $n = 14$, $*p = 0.024$, paired t-test), indicating that SST-IN activity could be influenced by GABA_ARs. However, pharmacological suppression of GABA_ARs did not enhance SST-IN activity, as firing rates were similar in control ACSF (0.80 ± 1.60 Hz) and after bath application of GABA_AR antagonist CGP (Fig. 1C,D; 1.19 ± 1.44 Hz, $n = 12$, n.s. $p = 0.333$, paired t-test). Thus, under our experimental condition GABA_ARs are not a prominent regulator of SST-IN activity and SST-IN spontaneous firing is not modulated by tonic activity of GABA_ARs. In contrast, excitatory transmission between L2/3 pyramidal neurons is tonically suppressed by GABA_ARs in this experimental condition indicating some tonic GABA_AR activation in vitro¹⁰.

Because GABA_AR agonists reduced the spontaneous firing of SST-INs, we asked whether this was via suppressing excitatory drive or decreasing the intrinsic excitability of these cells. First, we determined that excitatory synaptic drive contributes to SST-IN firing under our experimental conditions, since application of AMPA receptor and NMDA receptor antagonists (DNQX and APV) decreased spontaneous firing of SST-INs by 39% from 4.23 ± 3.0 Hz in control to 2.59 ± 2.3 Hz in antagonists (Fig. 1E,F; $n = 10$, $*p = 0.006$, paired t-test; see also¹⁵).

Importantly, when glutamate receptors were blocked, subsequent bath application of the GABA_AR agonist baclofen did not further influence spontaneous firing frequency in SST-INs (Fig. 1E,F; 2.57 ± 2.44 Hz in baclofen, $n = 10$, n.s. $p = 0.939$, paired t-test). Thus, GABA_ARs control SST-IN activity indirectly via the regulation of glutamatergic synaptic drive. This might be due to regulation of presynaptic release at Pyr-SST synapses, or by more complex circuit level effects^{21,22}.

To confirm that GABA_ARs regulate SST-IN activity only indirectly, via reducing excitatory synaptic drive to SST-INs but not the intrinsic excitability of these interneurons, we compared responses to somatic current injections before and after the application of GABA_AR agonists and antagonists (Fig. 2). Neither baclofen nor CGP influenced SST-IN intrinsic excitability, because there were no differences in the I-F curve (Fig. 2B,E), rheobase current (Fig. 2C,F; in baclofen $n = 17$, n.s. $p = 0.553$; in CGP $n = 12$, n.s. $p = 0.571$, paired t-test), and maximal frequency (in baclofen $n = 17$, n.s. $p = 0.375$; in CGP $n = 12$, n.s. $p = 0.806$, paired t-test). Also, neither input resistance nor resting membrane potentials of SST-INs were altered after drug application (Table 1). These data indicate that GABA_ARs do not modulate the intrinsic excitability of SST-INs.

To examine whether the GABA_AR-mediated suppression of SST-IN activity might occur via direct regulation of excitatory inputs onto these cells, we examined sEPSCs under low network activity conditions in regular ACSF (Fig. 3A–C). Since Pyr firing is negligible under these conditions^{10,18}, sEPSCs might be roughly equivalent to mEPSCs. The GABA_AR agonist baclofen indeed suppressed the frequency of sEPSCs by 25%, from 1.16 ± 0.44 Hz in control to 0.88 ± 0.34 Hz in baclofen (Fig. 3C; $n = 7$, $*p = 0.019$, paired t-test). Consistent with the assumption that sEPSCs are equivalent to mEPSCs, baclofen had no effect on EPSC amplitude. These data suggest that GABA_ARs might regulate the activity or release properties of local Pyr neurons. Application of CGP after baclofen was sufficient to restore sEPSC frequency to control values (Fig. 3A–C; 1.22 ± 0.47 Hz, n.s. $p = 0.712$, paired t-test ctrl vs. CGP). The renormalization of sEPSC frequency to control values after CGP indicates that GABA_ARs are not tonically activated when the network is largely silent, consistent with our previous findings¹⁰.

Then, we compared these effects to conditions where network activity was enabled in mACSF, since this is associated with higher levels of GABA release from the spontaneous firing of interneurons in the cortical network^{10,18}. Bath application of CGP now increased the frequency of sEPSCs recorded in SST-INs by 20% from 2.45 ± 0.59 Hz in control to 2.94 ± 0.62 Hz in CGP (Fig. 3D–F; $n = 7$, $*p = 0.019$, paired t-test) but not the sEPSC amplitude (Fig. 3E; 20.29 ± 1.87 pA in control and 19.63 ± 1.42 pA in CGP, n.s. $p = 0.664$, paired t-test).

In summary, these experiments suggest that GABA_ARs do not directly influence SST-IN activity through cell-autonomous mechanisms, but rather through regulation of excitatory inputs. The change in sEPSC frequency but not amplitude are consistent with modulation of presynaptic release properties at Pyr-SST synapses^{10,18}, although we cannot exclude other indirect network effects. The absence of GABA_AR modulation of SST-IN membrane properties and intrinsic excitability suggests that SST-IN activity may regulate network function independently,

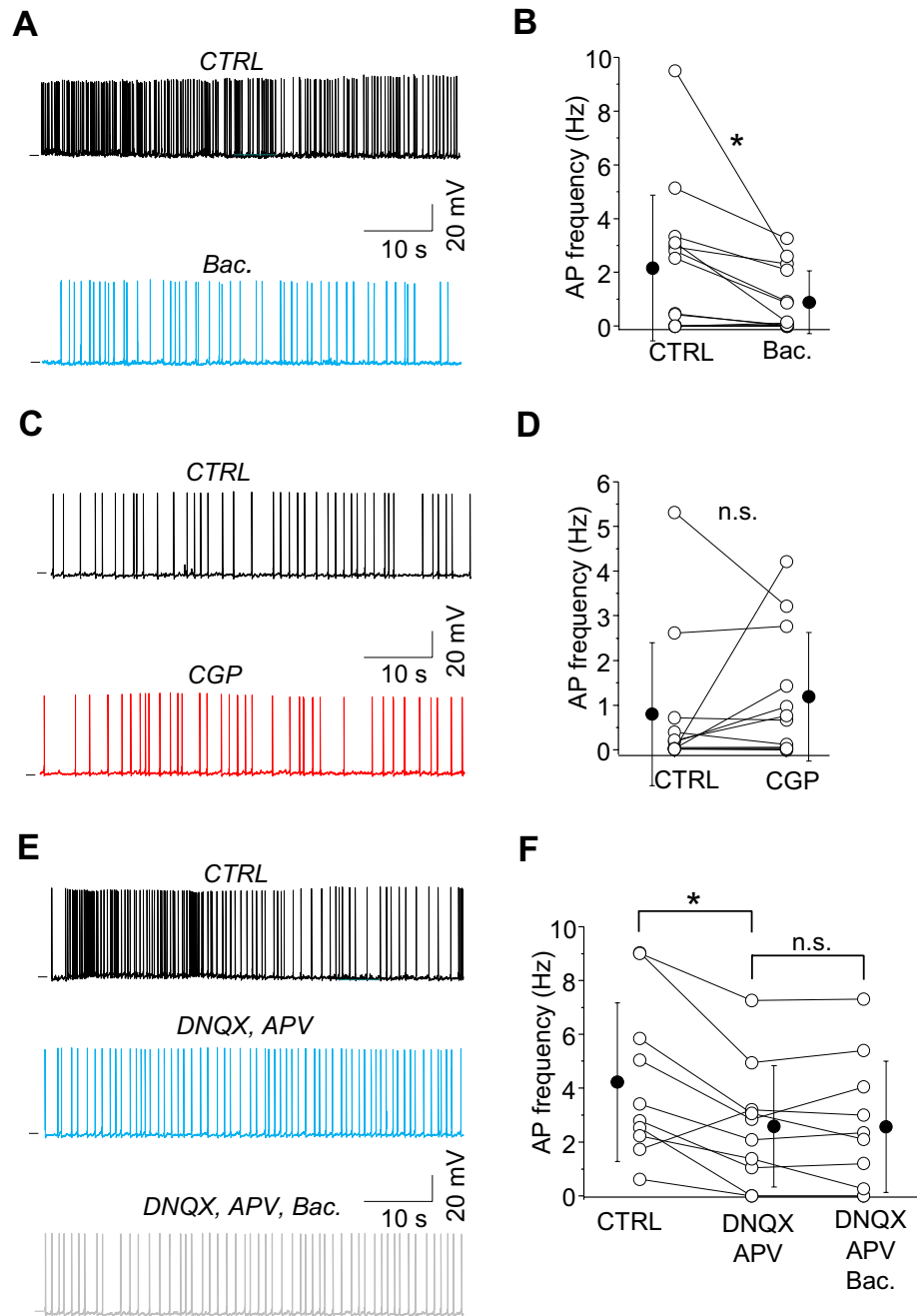


Figure 1. GABA_BRs regulate SST-IN spontaneous activity indirectly, via suppressing excitatory drive. **(A)** Example traces of SST-IN spontaneous firing in control (CTRL) mACSF followed by the application of GABA_BR agonist (baclofen, Bac.). **(B)** With-in cell comparison and mean (\pm SD) action potential (AP) firing of SST-INs in control and after baclofen (paired t-test, $*p=0.024$, $n=14$ cells). **(C)** The same as for **(A)** but for CTRL and after the application of GABA_BR antagonist CGP. **(D)** With-in cell comparison and mean (\pm SD) action potential (AP) firing of SST-INs in two conditions showing that AP frequency does not change when GABA_BR are blocked indicating that these receptors were not tonically activated in CTRL condition (paired t-test, n.s. $p=0.333$, $n=12$). **(E)** Example traces of SST-IN spontaneous firing in control mACSF (CTRL), after glutamatergic receptor antagonists (DNQX, APV) followed by the application of GABA_BR agonist (Bac.). **(F)** With-in cell comparison and mean (\pm SD) action potential (AP) firing of SST-INs in all three conditions (paired t-test, $*p=0.006$, n.s. $p=0.939$, $n=10$ cells).

without a negative feedback loop. To these ends, it is significant that SST neurons do not synapse onto each other, like other interneurons subtypes in the cortical network²³.

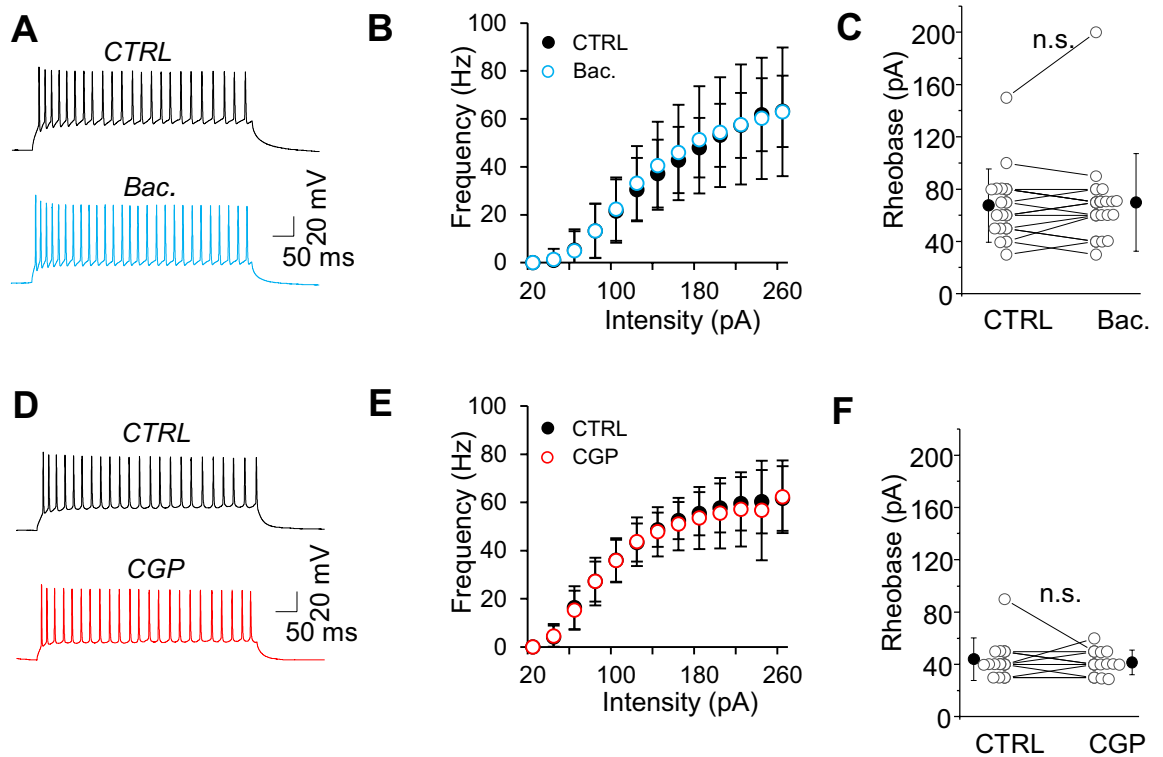


Figure 2. SST-IN intrinsic excitability is resistant to GABA_B modulation. (A) Example traces of firing responses after the somatic current injection of a 500 ms-long pulse (100 pA) in a cell recorded in CTRL rACSF followed by baclofen (Bac.). (B) Summary plot of the firing frequency (\pm SD) in response to current injections (from 0 to 270 pA) from SST-INs recorded in control ACSF and after baclofen (paired t-test, n.s., $n = 17$ neurons). (C) The comparison of mean (\pm SD) rheobase in control and baclofen (paired t-test, n.s. $p = 0.553$, $n = 17$). (D–F) The same as for (A–C) but for cells recorded in control mACSF followed by CGP (paired t-test, n.s. $p = 0.571$, $n = 12$ cells).

	CTRL	baclofen	p -value (n cells)	CTRL	CGP	p -value (n cells)
Membrane potential (mV)						
Pyr	-66.8 ± 4.9	-72.5 ± 3.8	*0.0001 (10)	-69.4 ± 4.7	-66.4 ± 7.0	*0.04 (9)
SST	-56.9 ± 5.3	-58.1 ± 3.5	0.176 (11)	-57.2 ± 4.4	-56.2 ± 4.9	0.103 (25)
PV	-63.1 ± 5.0	-65.4 ± 4.5	*0.00001 (19)	-62.9 ± 5.0	-60.3 ± 6.3	*0.004 (15)
Input resistance (M Ω)						
Pyr	380.2 ± 60.2	229.1 ± 50.3	*0.00001 (10)	206.3 ± 37.7	247.6 ± 58.7	*0.01 (9)
SST	384.3 ± 113.5	355.1 ± 109.4	0.073 (11)	336.0 ± 106.6	332.7 ± 113.3	0.789 (22)
PV	181.0 ± 48.2	156.1 ± 43.3	*0.00005 (19)	153.9 ± 42.5	180.7 ± 52.9	*0.0008 (15)

Table 1. Effects of GABA_B receptor pharmacological agents on membrane properties. mean \pm SD. *statistically significant.

SST-INs suppress L2/3 Pyr-SST synapses through GABA_B receptors. L2/3 Pyr neurons are densely connected to nearby SST-INs in primary sensory cortex (rev.;²³), although synaptic transmission from these connections is generally weak^{18, 24–26}. Excitatory connections between Pyr neurons can be silenced by presynaptic GABA_BRs, and the spontaneous firing of SST-INs is sufficient to suppress Pyr to Pyr (Pyr-Pyr) communication¹⁰. Here, we decided to examine whether spontaneous activity of SST-INs could also regulate excitatory drive onto SST-INs themselves. This is important, because it would indicate that when SST-IN activity is high (perhaps due to control by neuromodulators) they are unresponsive to sensory drive or local computations.

First we determined whether L2/3 Pyr-SST synapses could be regulated by GABA_BRs. Using dual patch-clamp recording, we established synaptically connected Pyr-SST pairs in L2/3 of the somatosensory cortex in a mouse brain slice in mACSF (Fig. 3G–I). Bath application of the GABA_B blocker CGP reduced failure rates of Pyr-SST EPSPs by 26% (Fig. 3I; from 0.73 ± 0.18 to 0.54 ± 0.29 ; $n = 7$, * $p = 0.045$, paired t-test) but did not change EPSP

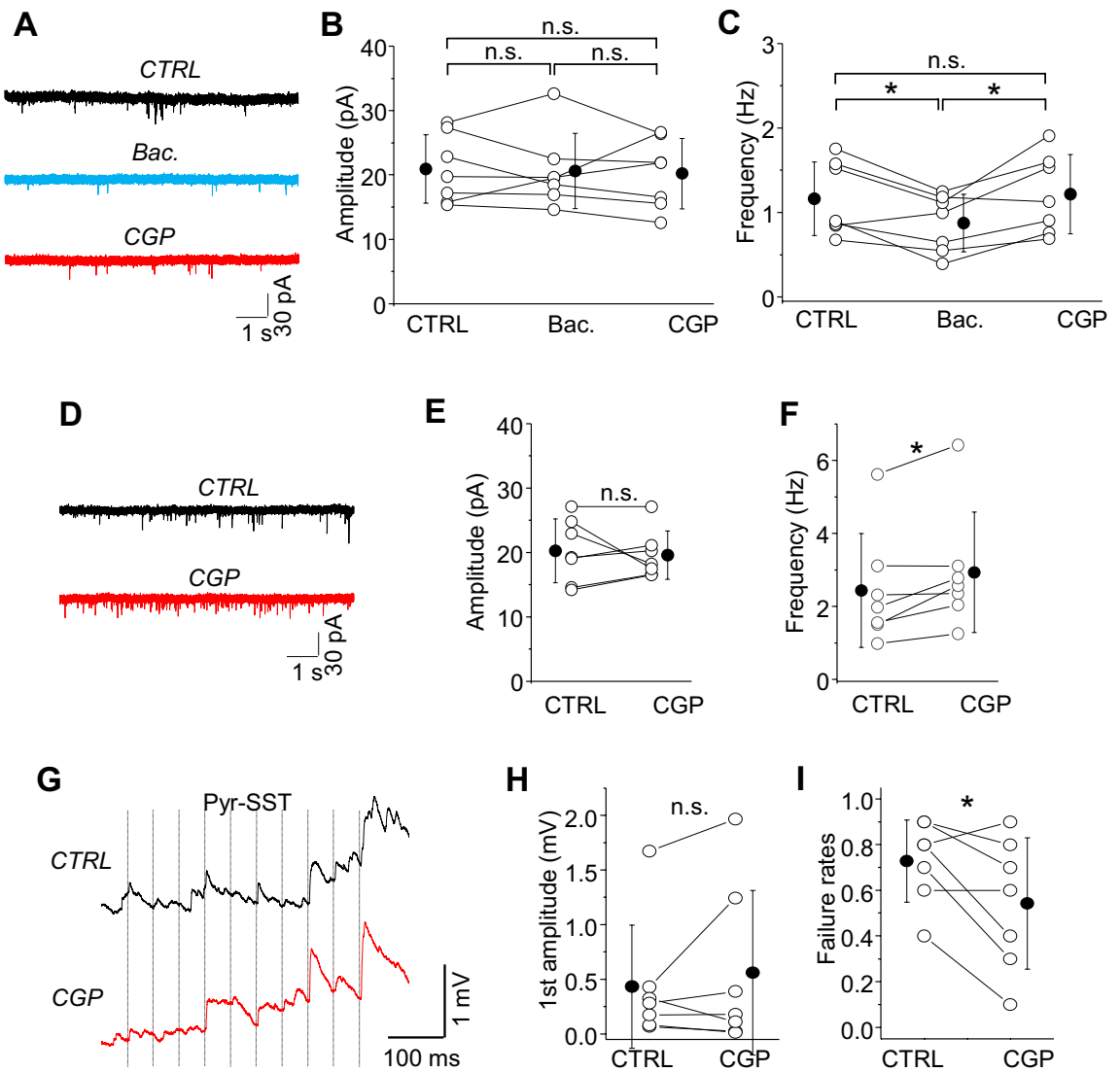


Figure 3. Presynaptic GABA_ARs decrease the frequency of sEPSCs in SST-INs and increase the failure rates at Pyr-SST synapses. **(A)** Example traces of sEPSCs recorded in rACSF in control and after GABA_AR agonist (Bac.) followed by GABA_AR antagonist (CGP). **(B)** With-in cell comparison and mean (\pm SD) amplitude of sEPSCs in SST-INs in all three conditions (paired t-test, $p=0.829$ ctrl vs. Bac., $p=0.808$ Bac. vs. CGP, $p=0.759$ ctrl vs. CGP, $n=7$ cells). **(C)** The same as for **(B)** but for the frequency of sEPSCs (paired t-test, $*p=0.019$ ctrl vs. Bac., $p=0.016$ Bac. vs. CGP, n.s. $p=0.712$ ctrl vs. CGP, $n=7$ cells). **(D)** Example traces of sEPSCs recorded in mACSF in control and after GABA_AR antagonist (CGP). **(E)** The mean (\pm SD) amplitude of sEPSCs was not different between ctrl and CGP (paired t-test, n.s. $p=0.664$, $n=7$ cells). **(F)** The mean (\pm SD) frequency of sEPSCs was higher in CGP than in control (paired t-test, $*p=0.019$, $n=7$) indicating that GABA_ARs are tonically active in mACSF. **(G)** The averaged trace of 10 response trials for a synaptic connection from a L2/3 Pyr neuron to an SST-IN (Pyr-SST) under baseline condition and in the presence of the GABA_AR antagonist (CGP). Ten presynaptic spikes (vertical lines) at 20 Hz were delivered. **(H)** With-in cell comparison and mean (\pm SD) EPSP amplitude in response to the first spike in the train, for baseline and in CGP conditions (Wilcoxon test, n.s. $p=0.578$, $n=7$ cells). **(I)** The same as for **(H)** but for failure rates (paired t-test, $*p=0.045$, $n=7$).

amplitude, consistent with the low release probability at these synapses (Fig. 3H; 0.43 ± 0.56 mV in control and 0.56 ± 0.75 mV in CGP, n.s. $p=0.578$, Wilcoxon test).

To check whether SST-IN firing can also regulate Pyr-SST synapses, we optogenetically suppressed SST-IN spontaneous activity (Fig. 4) using transgenic expression of the hyperpolarizing pump (Arch) in SST-Cre mice. Using paired whole-cell recordings of synaptically connected Pyr-SST, we tested whether acute silencing of SST-IN spontaneous activity might enhance EPSP strength and reliability of these connections. Illumination of the brain slice with yellow-green light (LED) for 1–1.5 s fully suppressed SST-IN firing, hyperpolarizing their membrane potentials by about 10–20 mV. During the light ON period, Pyr-SST EPSP failure rates were significantly reduced compared to OFF trials (Fig. 4D; 0.89 ± 0.11 mV in OFF and 0.77 ± 0.23 mV in ON, $n=13$, $*p=0.022$, paired t-test) and EPSP amplitude was not changed (Fig. 4C; 0.10 ± 0.15 mV in OFF and 0.20 ± 0.36 mV in ON,

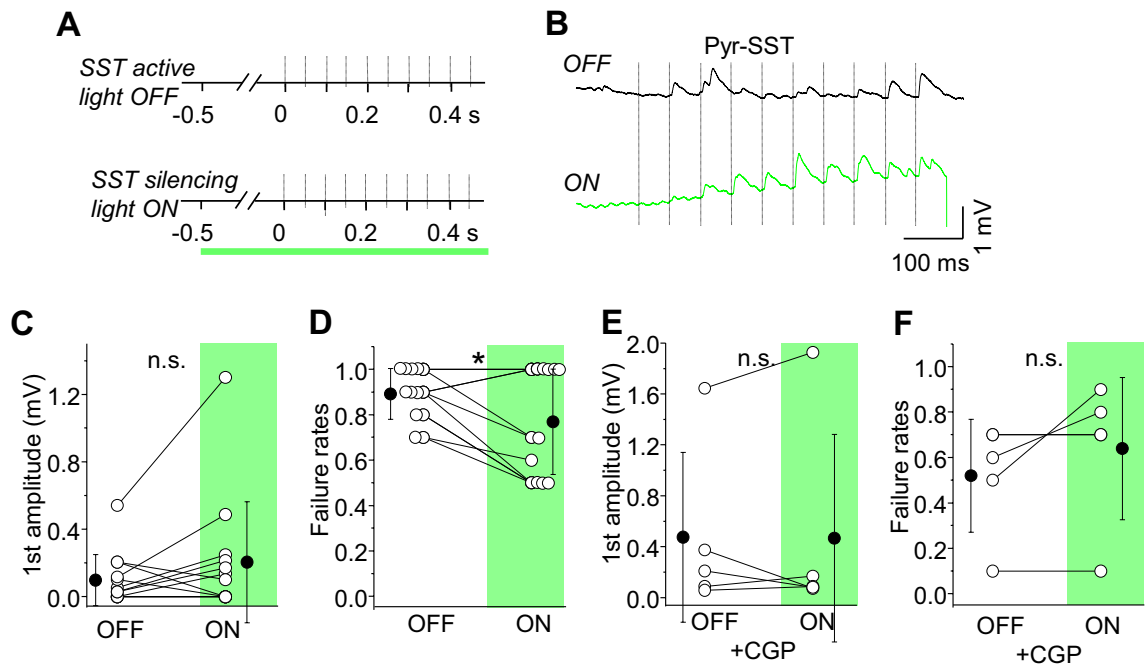


Figure 4. Somatostatin cell silencing enhances EPSP efficacy by reducing failure rates. **(A)** Schematic of the stimulation protocol. 1-second green light (1 s) was started 0.5 s prior to the presynaptic spike train. **(B)** The averaged trace of EPSP under baseline/light OFF and light ON conditions. **(C)** Within-cell comparison and mean (\pm SD) EPSP amplitude in response to the first spike in the train, for both conditions (paired t-test, *n.s.*, $n = 13$ cells). **(D)** Within-cell comparison and mean (\pm SD) failure rates after the first spike, for both conditions (paired t-test, $*p = 0.022$, $n = 13$). **(E)** and **(F)** The same as **(C)** and **(D)** but in the presence of the GABA_B receptors antagonist (paired t-test, *n.s.*, $p = 0.994$, $p = 0.208$, $n = 5$ cells).

$n = 13$, *n.s.*, $p = 0.15$, paired t-test). Thus, the effect of SST-IN silencing is consistent with the pharmacological results of GABA_BR manipulation, where EPSP failure rates were reduced in the presence of GABA_BR antagonists (Fig. 3G–I).

To confirm that this effect was due to GABA_BRs, we analyzed the effect of SST-IN silencing when GABA_BRs were blocked by CGP (Fig. 4E,F). Under these conditions, SST cell silencing did not change EPSP failure rates (Fig. 4F; 0.52 ± 0.25 mV in OFF and 0.64 ± 0.31 mV in ON, *n.s.*, $p = 0.208$, paired t-test) or amplitude (Fig. 4E; 0.48 ± 0.67 mV in OFF and 0.47 ± 0.82 mV in ON, $n = 5$, *n.s.*, $p = 0.994$, paired t-test), indicating that the effect was fully mediated by these receptors.

No tonic activation of presynaptic GABA_BRs at SST-IN output onto Pyr neurons. GABA released from SST-INs drives fast, GABA_AR-mediated, synaptic inhibition of postsynaptic neurons. The activation of presynaptic GABA_BRs at inhibitory terminals (so-called autoreceptors) can suppress GABA release and thus reduce synaptic inhibition¹². Do SST-INs also possess presynaptic GABA_BRs at synapses onto Pyr neurons? SST-INs to Pyr (SST-Pyr) connections are very common, where the L2/3 connection probability reached 60% (45 connected pairs out of 75 tested), consistent with other reports^{27, 28}.

Using paired whole-cell recordings of connected SST and Pyr neurons (SST-Pyr), we compared the effects of GABA_BR agonist (baclofen) on IPSC. Bath application of baclofen decreased the first IPSC amplitude by 84% (Fig. 5A,B; control 79.94 ± 46.49 pA vs. baclofen 13.09 ± 5.35 pA; $n = 5$, $*p = 0.031$, paired t-test) but had no effect on failure rates (Fig. 5C; 0.00 ± 0.00 in control to 0.04 ± 0.05 in baclofen, *n.s.*, $p = 0.5$, Wilcoxon test). Wash-on of CGP reversed the effects on IPSC amplitude to control values (Fig. 5B; 72.87 ± 29.12 pA in CGP, *n.s.*, $p = 0.654$ ctr vs. CGP, paired t-test). There was no effect on failure rates, since synaptic efficacy was high at these connections (Fig. 5C; CGP 0.0 ± 0.0 , *n.s.*, $p = 0.5$, ctrl vs. CGP, Wilcoxon test). If there are presynaptic GABA_BRs at SST-IN terminals, we predicted that the GABA_BR agonist baclofen would increase the paired-pulse ratio of the second response to the first (PPR) at SST-Pyr synapses. In superficial layers of the neocortex, SST-Pyr synapses are typically depressing, but this was shifted to a mild facilitation after the application of baclofen (Fig. 5D; control 0.51 ± 0.20 versus baclofen 1.10 ± 0.15 ; $*p = 0.017$, paired t-test), indicating a presynaptic locus of drug action. Subsequent bath application of the GABA_BR antagonist CGP reversed this facilitation back to control levels (Fig. 5D; 0.56 ± 0.11 in CGP, *n.s.*, $p = 0.661$, paired t-test), suggesting that GABA_BR activation was negligible under our recording conditions and consistent with the results obtained for SST-INs in the hippocampus²⁹.

Because the agonist was effective at reducing neurotransmitter release at SST-Pyr synapses, we asked whether presynaptic GABA_BRs might sometimes be activated by the synapse's own GABA release. In this case, the amplitude of the IPSC might be suppressed when neocortical SST neurons fire at some regular frequency, as has been described *in vivo* during the quiet resting state^{8, 20} and also *in vitro*, in mACSF^{10, 15, 18}. We thus examined the

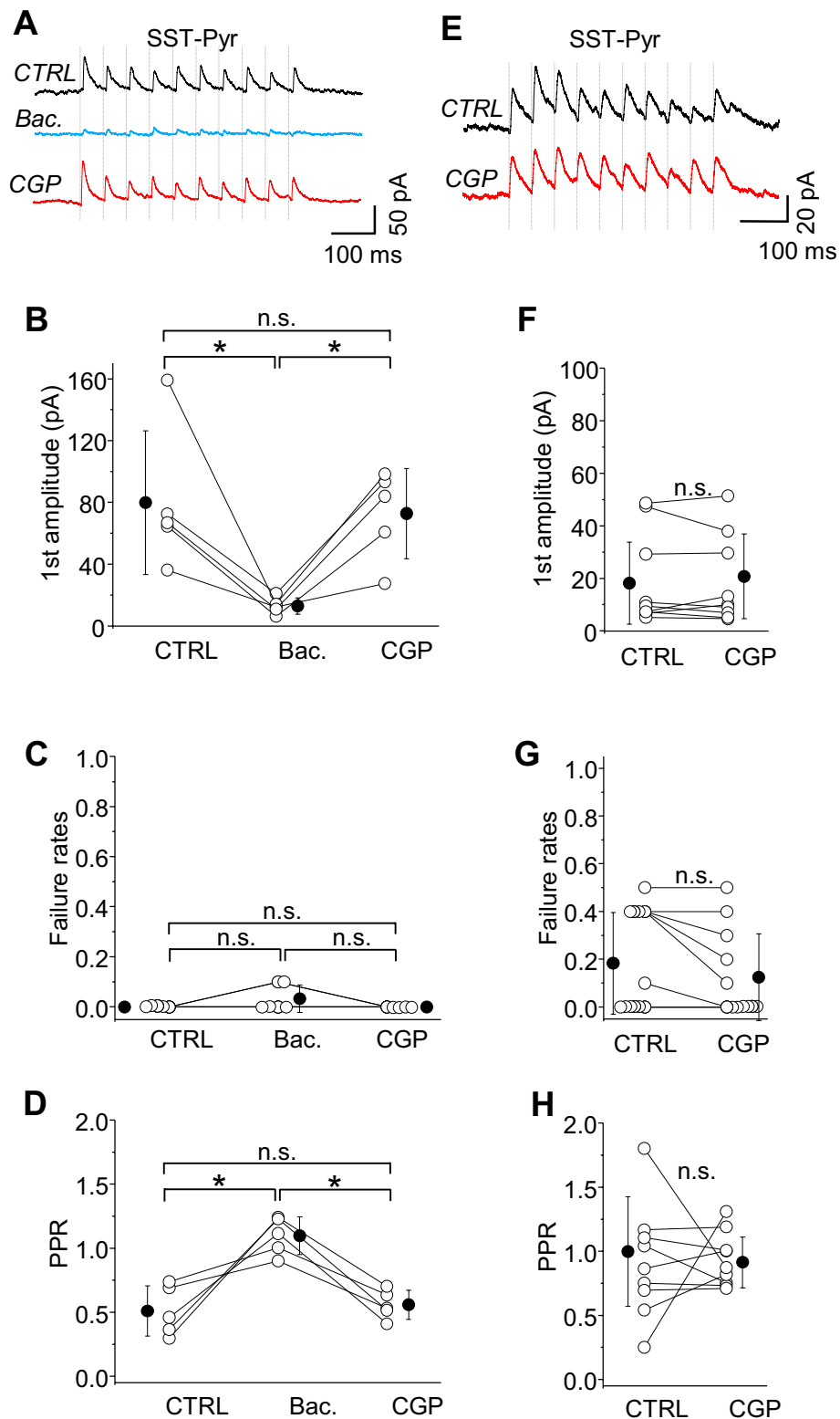


Figure 5. SST-IN outputs to Pyr neurons are not regulated by tonic activity of GABA_ARs. **(A)** The averaged trace of 10 response trials for a paired recording of a synaptic connection from an SST-IN to a L2/3 Pyr neuron (SST-Pyr) in control rACSF followed by baclofen and CGP. Ten presynaptic spikes (vertical lines) at 20 Hz were delivered. **(B)** With-in cell comparison and mean (\pm SD) IPSC amplitude in response to the first spike in the train, for control, baclofen and in CGP conditions (paired t-test, $*p=0.031$ ctrl vs. Bac.; $*p=0.008$ Bac. vs. CGP; n.s. $p=0.654$ ctrl vs. CGP; n=5). **(C)** The same as for **(B)** but for failure rates (paired t-test, n.s. $p=0.178$ ctrl vs. Bac; n.s. $p=0.178$ Bac. vs. CGP; Wilcoxon test, n.s. $p=0.5$ ctrl vs. CGP; n=5). **(D)** The same as for **(B)** but for PPR (paired t-test, $*p=0.017$ ctrl vs. Bac.; $*p=0.002$ Bac. vs. CGP; Wilcoxon test, ctrl vs. CGP n.s. $p=0.5$; n=5). **(E)** The averaged trace of 10 response trials for a paired recording of a synaptic connection from an SST-IN to a L2/3 Pyr neuron (SST-Pyr) in control mACSF and in CGP. Ten presynaptic spikes (vertical lines) at 20 Hz were delivered. **(F)** With-in cell comparison and mean (\pm SD) IPSC amplitude in response to the first spike in the train, for control and in CGP conditions (paired t-test, n.s. $p=0.252$, n=12 cells). **(G)** The same as for **(F)** but for failure rates (Wilcoxon test, n.s. $p=0.125$, n=12 cells). **(H)** The same as for **(F)** but for PPR (paired t-test, n.s. $p=0.558$, n=12 cells).

IPSC of connected SST and Pyr neurons in mACSF (Fig. 5E–H). Under baseline conditions, the evoked IPSC had a relatively low failure rate (0.18 ± 0.21 , $n = 12$, Fig. 5G) indicating that GABA_AR-dependent inhibition from SST-INs is strong even when spontaneous network activity is high. Bath application of CGP did not alter IPSC amplitude (Fig. 5F; control 18.28 ± 15.65 pA vs. CGP 20.82 ± 16.08 pA, $n = 12$, n.s. $p = 0.252$, paired t-test), failure rates (Fig. 5G; control 0.18 ± 0.21 vs. CGP 0.13 ± 0.18 , n.s. $p = 0.125$, Wilcoxon test) or PPR (Fig. 5H; control 1.00 ± 0.43 vs. CGP 0.92 ± 0.20 , n.s. $p = 0.558$, paired t-test). Altogether, these data indicate that although SST-INs have presynaptic GABA_BRs, spontaneous network activity may not be sufficient to activate these receptors.

Importantly (and in contrast to Pyr neurons), we did not observe any changes in resting membrane potential nor input resistance of SST-INs when GABA_BRs were either activated or blocked pharmacologically (Table 1). These data indicate that GABA_BRs in neocortical SST-INs are unlikely to act through potassium channels, similarly what has been observed for SST-INs in the hippocampal network³⁰.

To confirm that the spontaneous activity of SST-IN is not sufficient for the tonic activation of GABA_BRs at SST-Pyr synapses, we optogenetically silenced SST-INs to check whether it influences SST-Pyr connections (Supplementary Fig. 1). Analysis of SST-Pyr synapses showed that SST-IN silencing changed neither IPSC amplitude (Supplementary Fig. 1A–C; OFF 28.31 ± 21.74 pA vs. ON 28.91 ± 25.59 , $n = 5$, n.s. $p = 0.787$, paired t-test), nor failure rates (Supplementary Fig. 1D; 0.08 ± 0.13 in OFF and 0.10 ± 0.12 in ON, n.s. $p = 0.374$, paired t-test) nor PPR (Supplementary Fig. 1E; 0.79 ± 0.38 in OFF and 0.74 ± 0.11 in ON, n.s. $p = 0.827$, paired t-test). Thus, direct GABA_AR-mediated inhibition from SST-INs is not influenced by presynaptic GABA_BRs during spontaneous activity of SST-INs.

GABA_BRs modulate intrinsic excitability of L2/3 PV-INs in the neocortex. Does the spontaneous activity of SST-IN activate GABA_BRs on other neocortical neurons? Because PV neurons are a prominent source of inhibition in cortical networks^{26, 27, 31, 32}, we examined the effect of GABA_BR pharmacological modulation on both the intrinsic excitability of PV-INs (Fig. 6D–I) as well as Pyr to PV-IN inputs in L2/3 (Fig. 6A–C). GABA_BR activation using baclofen reduced the frequency of sEPSCs measured in PV-INs by 27% (Fig. 6A–C; control 3.45 ± 0.87 Hz vs. baclofen 2.52 ± 0.61 Hz, $n = 7$, $*p = 0.001$, paired t-test) but did not alter sEPSC amplitude (Fig. 6A–C; control 24.38 ± 8.52 pA vs. baclofen 20.96 ± 3.48 pA, n.s. $p = 0.168$, paired t-test). CGP fully reversed these effects (Fig. 6A–C; amplitude in CGP 19.86 ± 3.66 pA, n.s. $p = 0.138$; frequency in CGP 3.46 ± 1.05 Hz, n.s. $p = 0.944$, ctrl vs. CGP, paired t-test). Since changes in the event frequency are associated with changes in neurotransmitter release, this result suggests that presynaptic GABA_BR at Pyr-PV synapses can modulate excitatory synaptic transmission to L2/3 PV-INs.

Next, we analyzed PV-IN intrinsic excitability. In contrast to SST-INs, pharmacological activation of GABA_BRs profoundly influenced the intrinsic membrane properties of PV neurons (Fig. 6D–I). Bath application of baclofen suppressed the I–F curve (Fig. 6D,E), increased rheobase current (Fig. 6F, control 170 ± 21.38 pA vs. baclofen 205 ± 47.51 pA, $n = 8$, $*p = 0.031$, paired t-test) and decreased maximal firing frequency (control 128 ± 36.41 Hz vs. baclofen 113 ± 32.07 Hz, $n = 8$, $*p = 0.008$, Wilcoxon test, data not shown). CGP had the opposite effect, increasing evoked spiking with current injection (Fig. 6G,H), decreasing rheobase current (Fig. 6I; control 107.50 ± 39.90 pA vs. CGP 95.00 ± 39.64 pA, $n = 8$, $*p = 0.049$, paired t-test), although there was no effect on maximal firing frequency (control 132.00 ± 40.95 Hz vs. CGP 135.00 ± 23.77 Hz, n.s. $p = 0.816$, paired t-test, data not shown). Thus, unlike SST-INs, spontaneous network activity is associated with tonic GABA_BR activation in PV-INs that significantly suppresses the activity of these interneurons.

The reduction in PV-IN excitability was associated with significant GABA_BR modulation of Vrest. Resting membrane potential was hyperpolarized by ~ 2 mV by baclofen and depolarized by ~ 2 mV with CGP, and input resistance was decreased by baclofen and increased with CGP (Table 1). In contrast, both parameters in SST-INs showed no significant difference between control and drug applications (Table 1). These data suggest that postsynaptic GABA_BRs are coupled to potassium channels in PV- but not SST-INs³⁰.

GABA_BR-mediated suppression of PV-IN output onto Pyr neurons. GABA_BRs on PV-INs might primarily control the intrinsic membrane properties of these cells, or they also can directly regulate synaptic release. To determine whether L2/3 PV-IN terminals have presynaptic GABA_BRs, we examined the effects of GABA_BR antagonist on PV-IN-mediated IPSCs in Pyr neurons using paired whole-cell recordings (Fig. 7). PV-Pyr connections are extremely abundant in L2/3^{1, 28}, and we also observed that the probability of PV-Pyr connections reached 82% (9 connected pairs out of 11 tested). When network activity was high (in mACSF), we observed that IPSC failure rates were very low (0.05 ± 0.08 pA, $n = 8$, Fig. 7C), indicating that the efficacy of PV-Pyr synapses was very high even in the presence of high spontaneous firing of SST-INs. Bath application of the GABA_BR antagonist CGP increased IPSC amplitude by 48% (Fig. 7A,B; control 51.09 ± 37.44 pA vs. CGP 69.70 ± 51.36 pA, $n = 8$, $*p = 0.035$, paired t-test). Because failure rates were already negligible, CGP had no effect (Fig. 7C; 0.00 ± 0.00 in CGP, n.s. $p = 0.250$, Wilcoxon test). PPR decreased from 0.89 ± 0.11 in control to 0.76 ± 0.19 in CGP (Fig. 7D; $n = 8$, $*p = 0.043$, paired t-test). The effects of CGP on IPSC amplitude and PPR indicate that fast inhibition from PV-INs is modulated by tonic activity of presynaptic GABA_BRs under spontaneous network activity in acute brain slices.

Tonic GABA_BR activity in PV-INs is not regulated by spontaneous activity of SST-INs. SST-INs inhibit cortical networks directly, via fast synaptic transmission. In addition, through their spontaneous activity they also suppress communication between Pyr neurons via GABA_BRs¹⁰. To determine whether the spontaneous activity of SST-INs can activate GABA_BRs at synapses onto and from PV-IN, we crossed PV-Tdt mice with SST-Cre mice and virally transduced ArchT into SST cells.

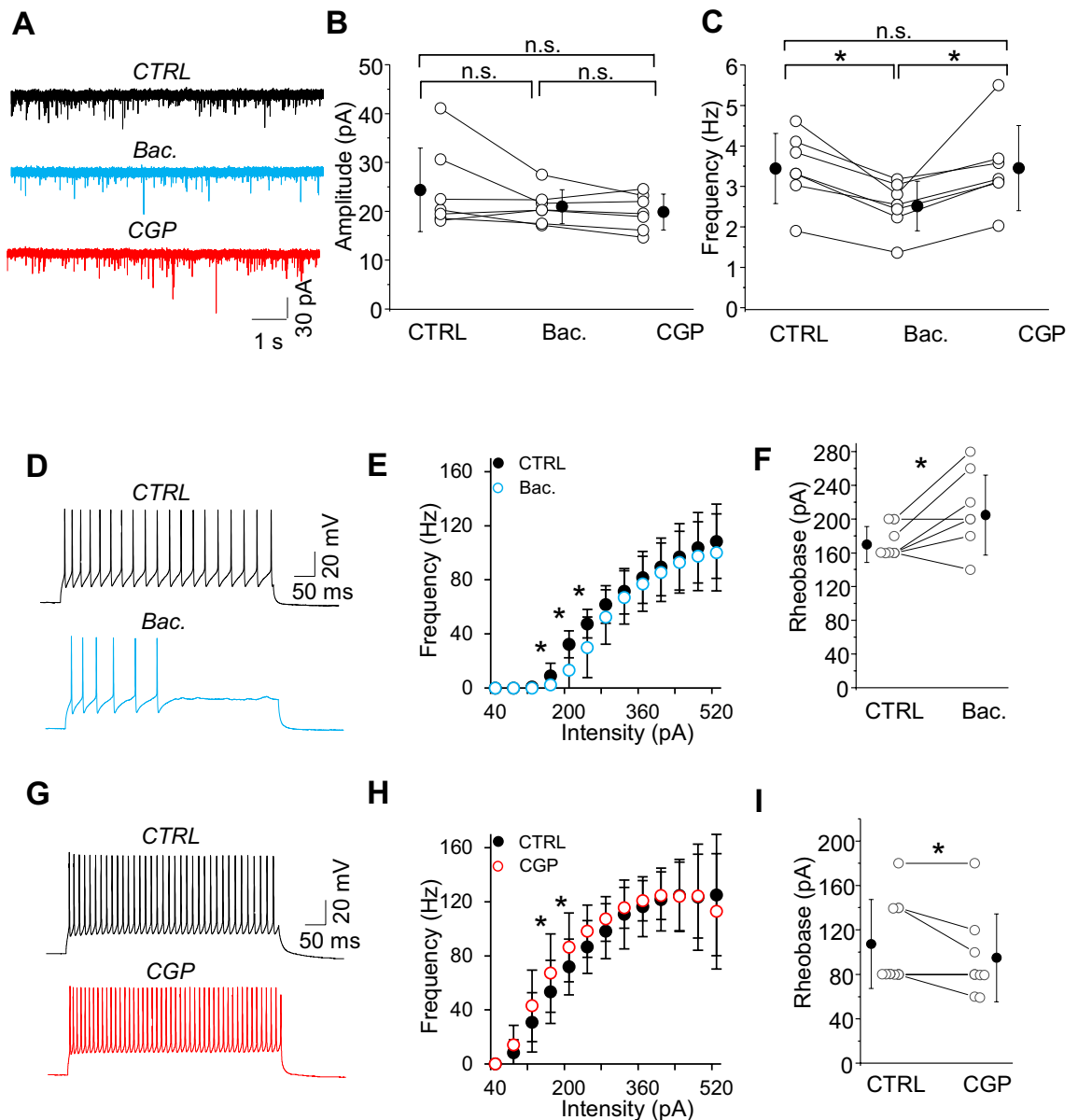


Figure 6. GABA_BR modulation of excitatory synaptic drive to PV-INs and their intrinsic excitability. (A) Example traces of sEPSCs recorded in rACSF in control and after GABA_BR agonist (Bac.) followed by GABA_BR antagonist (CGP). (B) Within cell comparison and mean (\pm SD) amplitude of sEPSCs in PV-INs in all three conditions (paired t-test, n.s. $p=0.168$ ctrl vs. Bac., n.s. $p=0.207$ Bac. vs. CGP, n.s. $p=0.139$ ctrl vs. CGP, $n=7$ cells). (C) The same as for (B) but for the frequency of sEPSCs (paired t-test, * 0.001 ctrl vs. Bac., 0.019 Bac. vs. CGP, n.s. 0.944 ctrl vs. CGP, $n=7$ cells) (D–I) The effect of GABA_BR pharmacological manipulations on PV-IN intrinsic excitability. (D) and (G) Example traces of firing responses after the somatic current injection of a 500 ms-long pulse (200 pA) in two separate cells recorded in control followed by baclofen (Bac.) and control followed by CGP, respectively. (E) Summary of the firing frequency (\pm SD) in response to current injections (from 0 to 550 pA) from PV-INs recorded in control ACSF and after baclofen (paired t-test, $n=11$). (H) The same as for (E) but for CGP (paired t-test, $n=8$ cells).

Using dual patch-clamp recordings, we tested whether acute silencing of SST-INs could change EPSP strength and reliability at both Pyr-PV and PV-Pyr synapses. SST-INs were silenced for 1 s before activation of Pyr-PV synapses (Fig. 8A,B). Surprisingly, SST-IN silencing had no effect on EPSP amplitude at Pyr-PV connections (Fig. 8C; OFF 0.30 ± 0.26 vs. ON 0.36 ± 0.32 mV, $n=7$, n.s. $p=0.337$, paired t-test). Also, failure rates and PPR at Pyr-PV synapses were not statistically different in light OFF and ON conditions (Fig. 8D,E; failure rates 0.49 ± 0.26 in OFF and 0.47 ± 0.34 in ON; PPR 1.10 ± 0.06 in OFF and 1.10 ± 0.98 in ON, n.s. $p=0.766$ and $p=0.999$, respectively). Similarly, IPSP amplitude, failure rates and PPR at PV-Pyr connections were not changed when SST-IN activity was optogenetically suppressed (Fig. 8F–J). IPSP amplitude was 1.30 ± 0.42 mV in light OFF and 1.20 ± 1.46 mV in light ON (Fig. 8H; $n=4$, n.s. $p=0.107$, paired t-test), failure rates were 0.00 ± 0.00 in OFF and ON conditions (Fig. 8I; n.s. $p=1$, paired t-test) and PPR was 0.72 ± 0.10 in OFF and 0.62 ± 0.25 in

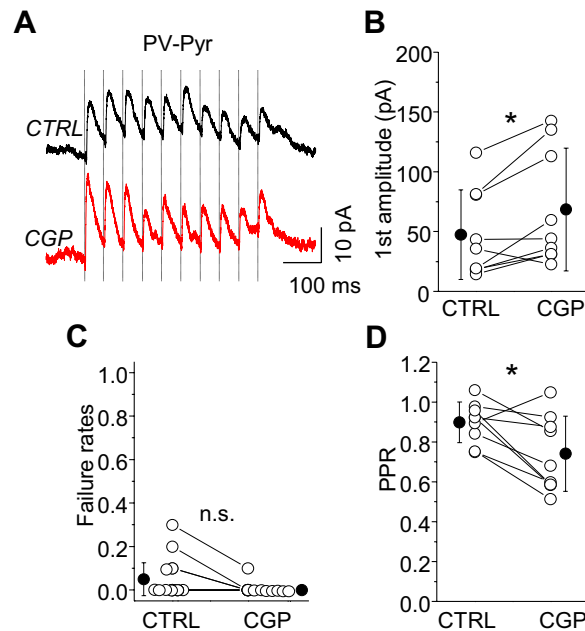


Figure 7. PV-Pyr synapses are regulated by tonic activity of GABAergic neurons. **(A)** The averaged trace of 10 response trials for a synaptic connection from a PV-IN to a L2/3 Pyr neuron (PV-Pyr) under baseline condition and in the presence of the GABAergic antagonist (CGP). Ten presynaptic spikes (vertical lines) at 20 Hz were delivered. **(B)** With-in cell comparison and mean (\pm SD) IPSC amplitude in response to the first spike in the train, for baseline and in CGP conditions (paired t-test, $*p=0.035$, $n=8$). **(C)** With-in cell comparison and mean (\pm SD) failure rates after the first spike, for both conditions (Wilcoxon test, n.s. $p=0.250$, $n=8$). **(D)** The same as for **(C)** but for PPR (paired t-test, n.s. $p=0.043$, $n=8$).

ON (Fig. 8J; n.s. $p=0.554$, paired t-test). These findings demonstrate that despite the presence of GABAergic neurons at excitatory synapses onto PV-INs as well as PV-INs outputs onto Pyr cell targets, SST-IN spontaneous firing is not sufficient to regulate these connections.

Discussion

GABAergic neurons regulate both synaptic transmission as well as membrane potential, and the tonic activation of GABAergic neurons can regulate synaptic function and overall network activity. Prior studies have shown that SST neurons are an important source of GABA that activates GABAergic neurons¹⁰. Here we investigate whether SST neurons themselves might be regulated by GABAergic neurons as a possible negative feedback loop in the cortical circuit using targeted whole-cell patch clamp recordings in acute brain slices. Pharmacological activation of GABAergic neurons reduced excitatory drive onto SST-INs to decrease SST-IN spontaneous activity, and optogenetic suppression of SST-IN activity was sufficient to enhance synaptic transmission at Pyr-SST synapses in a GABAergic-dependent manner. These data suggest that SST-IN firing is part of a negative feedback loop, by which the activity of SST-INs suppresses the effect of local excitatory input in further activating SST-INs. However, under network-active conditions where SST neurons are depolarized and their firing activity is high^{8, 10, 15, 19}, GABAergic antagonist application did not further enhance SST-IN firing activity. These results suggest that ambient GABA from spontaneous network activity may not be sufficient to regulate SST-IN firing output. In contrast, ambient GABA during spontaneous network activity could regulate synaptic properties of both excitatory inputs onto PV-INs as well as PV-IN synaptic output via GABAergic neurons. GABAergic neurons also controlled the intrinsic excitability of PV-INs. However, we determined that this tonic GABAergic activation was unlikely to come from SST-INs, since optogenetic silencing of SST neurons did not influence PV-IN-related synapses.

Altogether, our data indicate that GABAergic neurons modulate the activity of SST- and PV-INs in a different way. Under conditions of elevated spontaneous network activity, excitatory synaptic inputs to both SST- and PV-INs are depressed by tonic activity of GABAergic neurons, reducing the influence of local excitatory drive onto these inhibitory neurons to diminish network inhibition. This effect is enhanced by the fact that PV-IN-mediated feedback inhibition onto Pyr neurons is markedly reduced by the tonic activation of GABAergic neurons.

Both light and electron microscopic analysis of GABAergic immunoreactivity shows that these receptors are expressed in cell bodies, dendrites and terminals of most types of neurons in the neocortex and the hippocampus; however, the net effect of GABAergic neurons will depend upon the specific ion channels that they are linked to, leading to different effects on network function and connectivity. Canonically, postsynaptic GABAergic neurons activate G-protein-coupled inwardly-rectifying potassium channels (such as Kir-3), leading to hyperpolarization of the neuronal membrane and thus decreasing neuronal activity^{33–35}. However, consistent with the analysis of hippocampal SST-INs³⁰, we observed a moderate but not significant alteration in membrane potential and input resistance of

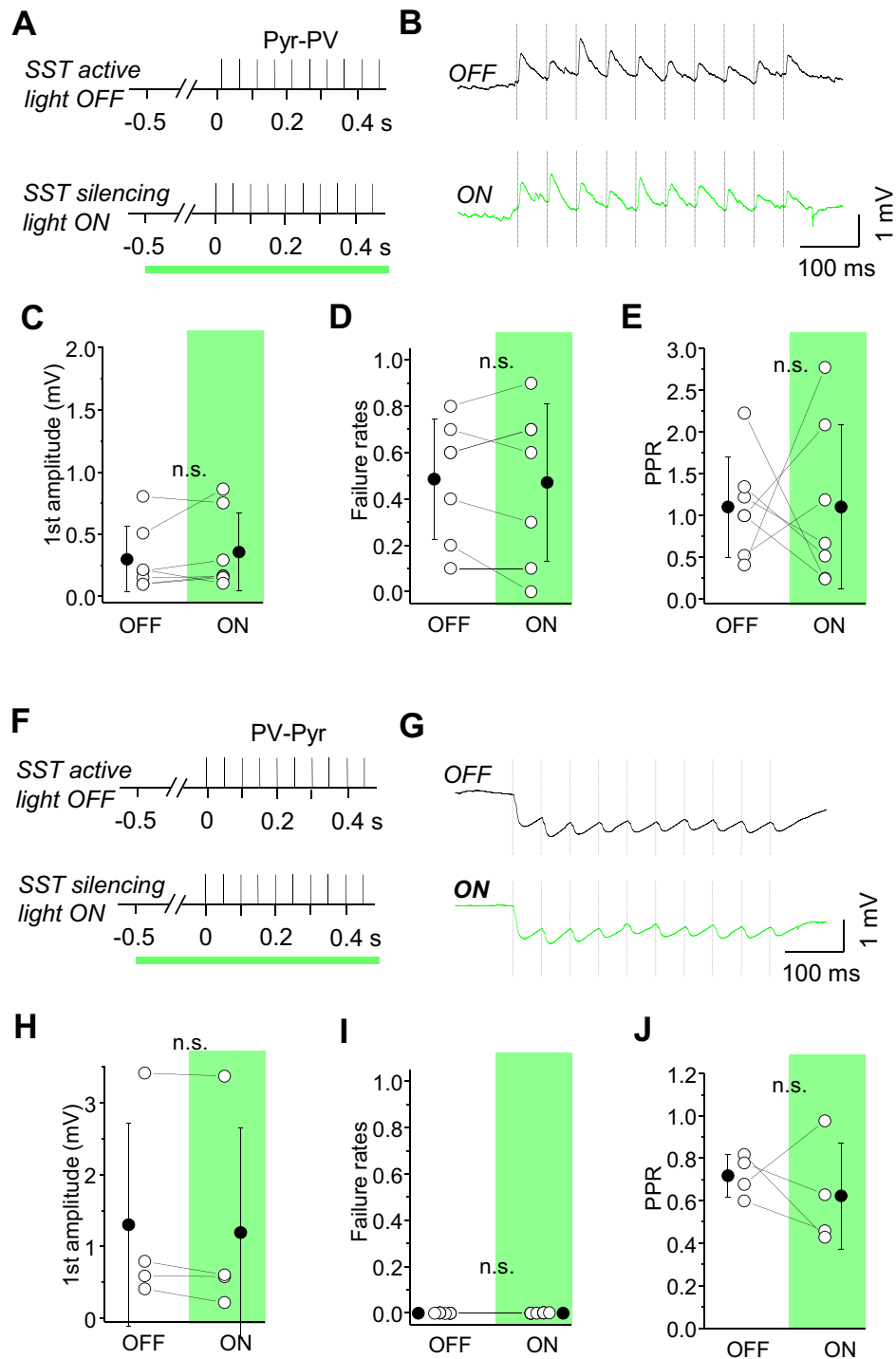


Figure 8. SST-IN spontaneous firing does not control inputs and outputs of PV-INs. **(A)** ArchrhodopsinT was expressed in SST-INs and Pyr to PV EPSP were analyzed in paired recordings. Schematic of the stimulation protocol. 1-second green light (1 s) was started 0.5 s prior to the presynaptic spike train. **(B)** An example of the averaged trace of EPSP under baseline/light OFF and light ON conditions. **(C)** Within-cell comparison and mean (\pm SD) EPSP amplitude in response to the first spike in the train, for baseline and light ON conditions (paired t-test, n.s. $p=0.337$, $n=7$). **(D)** Within-cell comparison and mean (\pm SD) EPSP failure rates for baseline and light ON conditions (paired t-test, n.s. $p=0.766$, $n=7$). **(E)** The same as for **(D)** but for PPR (paired t-test, n.s. $p=0.999$, $n=7$). **(F–J)** The same as for **(A–E)** but for IPSPs recorded in PV to Pyr connections (n.s. $p=0.107$, $p=1$, $p=0.554$, respectively, $n=4$).

L2/3 SST-INs after GABA_BR agonist and antagonist administration, suggesting that neocortical SST-INs possess postsynaptic GABA_BRs which are not strongly coupled to Kir channels. It is possible that GABA_BRs might be co-clustered with and inhibit L-type channels as observed in hippocampal SST-INs³⁰. In contrast to SST-INs, we found significant changes in the membrane potential and input resistance in L2/3 PV-INs and Pyr after the application of GABA_BR agonists and antagonists, indicating that postsynaptic GABA_BRs activate potassium channels on these neurons. Thus, the cell-type specific differences in pharmacological effects on resting membrane potential and input resistance between these cell types are due to the localization of Kir channels that are sensitive to GABA_BR modulation.

Presynaptic GABA_BRs, which can suppress the release of both glutamate and GABA, are widely distributed across the brain. However, it is unclear whether specific interneuron subtypes possess GABA_BRs that modulate synaptic release. Immunoreactivity for presynaptic GABA_BRs has been observed on hippocampal interneurons expressing SST, neuropeptide Y, calretinin, calbindin, or cholecystokinin (CCK) but not on PV-INs³⁶. Other studies that used electrophysiological recordings and freeze-fracture replica-based quantitative immunogold electron microscopy have revealed the presence of presynaptic GABA_BRs on hippocampal CCK and PV-INs¹⁴. Fast, GABA_AR inhibition from PV to Pyr neurons is weakly reduced by presynaptic GABA_BRs in the hippocampus^{14, 37, 38}; however, these effects may be region-specific since GABA_A-mediated inhibition from L5 fast-spiking (presumably PV) interneurons was strongly modulated by GABA_BRs³⁹. In developing gerbil auditory cortex, GABA_AR-mediated inhibition from L2/3 FS (presumably PV-INs), but not from LTS (presumably SST-INs) is controlled by presynaptic GABA_BRs⁴⁰. Our study showed that despite the fact that both SST- and PV-INs have presynaptic GABA_BRs (autoreceptors), only the fast inhibition from PV-INs is tonically suppressed through GABA_BRs, whereas fast inhibition mediated by SST-INs appears insensitive to GABA_BR tonic modulation. Thus, mechanisms for presynaptic GABA_BR modulation are region-specific, differing between hippocampal and neocortical interneurons.

In vitro recordings show that SST-INs can exhibit high levels of spontaneous activity that is independent of glutamatergic input or electrical stimulation¹⁵. Indeed, we find that local synaptic drive to SST-INs under our in vitro recording conditions is markedly low, consistent with ours and others' previous work^{rev., 23, 41}. Here we show that optogenetic silencing of SST-INs in these active network states enhanced synaptic input from Pyr to SST-INs, an effect that was dependent upon GABA_BRs. These data suggest that SST-IN inhibition may exist in two different regimes: one, where spontaneous SST-IN activity is temporally imprecise and has a more global effect on reducing functional coupling within the network, and the second where spontaneous activity of SST-INs is low and can be temporally synchronized to provide fast, feedback inhibition in the local network. Spontaneous activity of SST-INs thus reduces network activity in two separate ways: first, via direct and fast GABA_AR-dependent inhibition of downstream targets and second, via slow and indirect suppression of local synaptic transmission.

The conditions that enable spontaneous activity of SST-INs, where they are a significant source of ambient GABA that silences not only local excitatory transmission between Pyr neurons¹⁰ but also excitatory synapses onto SST-INs, will be of great interest to identify. It remains unknown under what brain states presynaptic GABA_BR are activated in SST-IN terminals in the neocortex; it is reasonable to hypothesize that this might happen during the states in which SST-IN activity is higher than during the quiet state.

Notably, GABA_BR-mediated inhibition by SST-INs is not global, as synaptic efficacy between Pyr neurons and PV-INs was not changed with optogenetic suppression of SST-IN activity. The second important finding of our study shows that fast synaptic inhibition mediated by SST-INs on to local Pyr cells is not suppressed by the tonic activity of presynaptic GABA_BRs. These data indicate that SST-INs might provide effective inhibition to the local network under high network activity conditions, in contrast to PV-INs which fast inhibition can be suppressed by tonic activity of GABA_BRs. Future studies will reveal the specific cellular source of GABA responsible for activating GABA_BR on SST- and PV-IN terminals.

Inhibitory interneurons play an essential role in controlling cortical activity at various temporal and spatial scales⁴². SST-INs preferentially inhibit distal parts of Pyr neurons whereas PV-INs synapse on the soma and proximal parts of the target neurons^{3, 4, 43}, regulating inputs and outputs of excitatory neurons, respectively. Here, we provide a functional comparison for the sensitivity of two main neocortical interneurons in the activation of GABA_BRs. Under conditions of high GABA release, the differential sensitivity of SST- and PV-INs to GABA_BR modulation will favor fast (GABA_AR) inhibition mediated by SST- over PV-INs. Our data show that the weak excitatory synaptic input onto SST-INs from local Pyr cells can be further reduced by the spontaneous activity of SST-INs. However, SST-INs can still generate powerful GABA_A-mediated inhibition thanks to their intrinsic spontaneous activity that is insensitive to GABA_BRs.

Because Pyr neurons receive not only local inputs from neighboring Pyr neurons within L2/3 but also from other cortical layers^{24, 25, 28, 44} as well as other brain areas^{45–47}, GABA_BR-mediated silencing of local inputs might shift the balance of control of L2/3 Pyr neurons from local to long-range inputs. Consistent with this, prior studies have shown that thalamocortical inputs to L4 excitatory neurons are resistant to GABA_BR modulation⁴⁸ but see³⁹. Thus, our data suggest that when SST-IN activity is high, local circuit amplification of incoming sensory information will be weak.

Pharmacological experiments for induction of synaptic plasticity in acute brain slices have yielded mixed results about the role of GABA_BRs. For example, in the hippocampus, GABA_BRs prevent the induction of long-term potentiation (LTP) in SST-INs³⁰ but can facilitate the induction of LTP in CA1 Pyr cells^{49, 50}, indicating that the effects of these receptors may be synapse-specific and also implicating these receptors in synaptic plasticity during learning and memory. In layer 4 (L4) of primary visual cortex of rats, the strengthening of synapses from FS cells (presumably PV-IN) to Pyr neurons requires the activity of postsynaptic GABA_BRs, although LTP between L4 excitatory cells was not affected by GABA_BR antagonists⁵¹. Critically, these pharmacological manipulations may not precisely recapitulate the tonic activation of GABA_BRs under more naturalistic activity conditions. It remains unknown whether LTP at other excitatory synapses is sensitive to GABA_BR activation, and

which interneurons may regulate plasticity at input- and target-specific synapses. Interestingly, recent studies have reported that dually innervated dendritic spines on hippocampal pyramidal neurons are resistant to structural plasticity due to tonic inhibition of NMDA receptors through GABA_BRs and SST-INs⁵².

Taken together, our data demonstrate that GABA_BRs modulate neocortical networks in a neuron- and synapse-specific manner (Supplementary Fig. 2). The differential sensitivity of specific synapses and neurons to GABA_BR-modulation may fine-tune the balance of excitation and inhibition in a compartment-specific manner, providing tight control of information flow to Pyr neurons in superficial layers.

Materials and methods

Ethical approval. All experimental procedures were conducted in accordance with the Act on the Protection of Animals Used for Scientific or Educational Purposes in Poland (Act of 15 January 2015, changed 17 November 2021; directive 2010/63/EU) and the National Institute of Health guidelines in USA. All experimental protocols were approved by Polish Ministry of Environment (Dec. No 47/2019) and the Institutional Animal Care and Use Committee at Carnegie Mellon University (Approval No PROTO201600045). The study was reported in accordance with ARRIVE guidelines.

Animals. Mice were housed under controlled light cycles (12-h light–dark cycles) with ad libitum access to food and water.

The following strains of mice were used: (1) Sst-IRES-Cre mice on a C57Bl6 background (Jackson Labs stock # 013044); (2) Pvalb-T2A-Cre-D on a C57Bl6 background (Jackson Labs stock #012358); (3) PValb-tdTomato-miGAD67 (Jackson Labs stock #028594); (4) Ai14 mice on a mixed background, C57Bl6] and B6;129S6 (Jackson Labs stock #007908); (5) Ai35D on a C57Bl6 background (Jackson Labs stock # 012735). Experiments were performed in offspring of Sst-IRES-Cre mice crossed to either Ai14 (floxed-Tdt) or Ai35D (floxed-Arch-YFP) reporter mice, in offspring of Pvalb-T2A-Cre-D mice crossed to Ai14, in offspring of PValb-tdTomato-miGAD67 crossed to Sst-IRES-Cre. All transgenes were used as heterozygotes and both sexes were used.

Virus injection. Virus injection procedures were performed at CMU and conducted with the NIH guidelines (USA) and approved by the Institutional Animal Care and Use at Carnegie Mellon University (Approval No PROTO201600045). New born (P0–1) double transgenic mice (Sst-IRES-cre: PValb-tdTomato-miGAD67) were injected with a flex-GFP-ArchT virus to the somatosensory cortex to optogenetically silence SST-INs. Mouse newborns were anesthetized by incubation on ice prior to virus injection. The virus (rAAV1/flex-ArchT-GFP, UNC Vector Core) was delivered using a glass micropipette (tip diameter 10–20 μm) attached to a picospritzer microinjector (WPI). In vitro electrophysiology experiments were conducted 18–25 days after virus injection.

Brain slice preparation. At the age of P18–P28, where P0 indicates the day of birth, mice were deeply anaesthetized with isoflurane and killed by decapitation using procedures in accordance with the Polish Animal Protection Act (Act of 15 January 2015, changed 17 November 2021; directive 2010/63/EU) and the NIH guidelines (USA).

Brain slices (350 μm thick) were prepared by an “across-row” protocol in which the anterior end of the brain was cut along a 45° plane toward the midline⁵³. Slices were recovered and maintained at 24 °C in regular artificial cerebrospinal fluid (ACSF) composed of (in mM): 119 NaCl, 2.5 KCl, 2 MgSO₄, 2 CaCl₂, 1 NaH₂PO₄, 26.2 NaHCO₃, 11 glucose equilibrated with 95/5% O₂/CO₂.

Whole-cell recording. To enable spontaneous firing of SST-INs and tonic activation of GABA_BRs, recordings were performed in modified ACSF (mACSF) solution composed of (in mM): 119 NaCl, 3.5 KCl, 0.5 MgSO₄, 1 CaCl₂, 1 NaH₂PO₄, 26.2 NaHCO₃, 11 glucose equilibrated with 95/5% O₂/CO₂, as described before^{10,18}. To prevent the network from spontaneous firing, a part of experiments were performed in regular ACSF (rACSF) where the following ingredients were changed to 2.5 KCl, 1.3 MgSO₄, 2.5 CaCl₂.

Somata of L2/3 neurons in primary somatosensory cortex were targeted for whole-cell recording with borosilicate glass electrodes, resistance 4–8 MΩ. For current clamp mode, electrode internal solution was composed of (in mM): 125 potassium gluconate, 2 KCl, 10 HEPES, 0.5 EGTA, 4 Mg-ATP, and 0.3 Na-GTP, at pH 7.25–7.35, 290 mOsm and contained trace amounts of Alexa 488 to verify the location of the recorded cell. For voltage clamp mode, electrode internal solution was composed of (in mM): 130 cesium gluconate, 10 HEPES, 0.5 EGTA, 8 NaCl, 10 tetraethylammonium chloride, 5 QX-314, 4 Mg-ATP, and 0.3 Na-GTP, at pH 7.25–7.35, 290 mOsm and contained trace amounts of Alexa 488.

Because of the difficulty in identifying connected pairs, the majority of recordings were carried out at room temperature (24 °C) to enable longer recording periods, since prolonged incubation at warmer temperatures degrades cell health and diminished recording quality.

Electrophysiological data were acquired by Multiclamp 700A or Multiclamp 700B (Molecular Devices) and digitized with a National Instruments acquisition interface or Digidata 1550B (Molecular Devices). The data were filtered at 3 kHz, digitized at 10–20 kHz and collected by Igor Pro 6.0 (Wavemetrics) or pClamp (Molecular Devices). Series and input resistances were analyzed online, recordings were discarded when access or series resistances were unstable more than 30%.

Neuron classification. Neurons were classified as Pyr neurons according to Pyr-like soma shape, the presence of an apical dendrite and spines visible after Alexa filling reconstruction as well as according to regular spiking in response to 500 ms suprathreshold intracellular current injection. SST-IN were identified using fluo-

rescent reporter gene expression in Sst-Cre::Ai14, whereas PV-INs were visualized by the fluorescent marker genetically encoded in Pvalb-T2A-Cre-D::Ai14 or PValb-tdTomato-miGAD67 mice. Additionally, the firing responses to the somata current injection were analyzed. SST-INs responded to current steps with low threshold spiking (LTS) firing with a spike-rate adaptation, and the AHP after the first action potential was more negative than the last AHP during the current step¹⁵. PV-INs were identified by fast-spiking (FS) firing with a non-adapting firing pattern and AHP magnitudes that were uniform throughout a given current step.

Connectivity analysis. Synaptically connected neurons were identified by paired whole-cell patch-clamp recordings. The distance between cells was $\leq 300 \mu\text{m}$. To evaluate Pyr to SST-IN connections (Pyr-SST) or Pyr to PV-IN (Pyr-PV), both cells were maintained in current clamp mode and EPSPs were recorded in SST- or PV-IN in response to the current injection to the presynaptic Pyr. Interneuron membrane potential was maintained at the hyperpolarized value about -60 mV to block spontaneous spiking activity of the recorded cell and to visualize EPSPs. To evaluate inhibitory interneuron to Pyr connections, the membrane potential of an interneuron was maintained in current clamp, whereas the postsynaptic cell was kept in voltage clamp at the holding potential of 0 mV to record IPSCs in the response to the presynaptic spikes evoked by the current injection. Alternatively, IPSPs were recorded in current clamp mode at the depolarizing membrane potential of about -55 mV . To assess connectivity, we analyzed responses from 20 trials delivered at 0.1 Hz of a 10-stimulus spike train ($3\text{--}5 \text{ ms}$ long, 1 nA at 20 Hz). The 10-spike train was critical for accurate assessment of synaptic connections, since weak and facilitating connections (such as at Pyr to SST-IN synapses) cannot be detected with single spikes²⁸. Evoked postsynaptic responses were calculated using responses from 10 trials of the stimulus train. To precisely identify the onset of the synaptic response, analysis was focused on events that occurred during DOWN-states, since responses during UP-states were difficult to isolate from background activity in the sweep⁵⁴. Because in vivo, L2/3 Pyr neurons rarely respond more than a single spike and almost never at frequencies exceeding 20 Hz ⁵⁵, we considered responses to the first presynaptic spike to be most representative of synaptic function as it might occur during normal sensory-evoked activity. Thus, amplitude and failure rate measurements are plotted for the EPSP (or IPSC/P) evoked by the first stimulus in the spike train.

Spontaneous excitatory postsynaptic currents (sEPSCs) were recorded in voltage clamp at -70 mV . Spontaneous firing was recorded at the resting membrane potentials without any correction. Spontaneous activity was analyzed within at least 3 min of current-clamp recordings in control ACSF and ACSF with agents.

Intrinsic excitability was accessed using square pulses of 500 ms of increasing amplitude up to maximal firing frequency (steps of 10 pA and 20 pA , for SST- and PV-INs, respectively). To control for potential effects of GABA_BR agents on Vrest, the membrane potential of interneurons was maintained at -65 mV across different pharmacological conditions.

Pharmacology. The GABA_B receptor antagonist (CGP 55845, $1 \mu\text{M}$) and agonist (baclofen, $10 \mu\text{M}$), as well as the AMPAR antagonist (DNQX, $20 \mu\text{M}$) and NMDAR antagonist (APV, $50 \mu\text{M}$) were bath applied for at least 10 min before data acquisition to assess drug effect for 20 trials of the 10-pulse train. All the pharmacological agents were purchased from Tocris.

Optical stimulation. For ArchT activation, photo stimulation was produced by a light-emitting diode (white LED with 590 nm filter set to maximum range, Prizmatix, Israel) and delivered through a $40\times$ water-immersion objective. After establishing a connection, SST-IN silencing was initiated 1 s or 1.5 s prior to the 10 pulse presynaptic train and maintained to the end of the spike train. Because the light hyperpolarized the membrane potential of SST-INs, the light ON trials were collected before light OFF trials (20 repetitions at 0.1 Hz for both periods). The light OFF trials were collected at the membrane potential of SST-INs adjusted by the constant somata current injection to the same value as it was during light ON period.

Data analysis. Population data are presented as mean \pm SD. 1–2 cells or 1 synaptically connected pair were analyzed in an individual mouse. Statistical significance was defined as $p < 0.05$ using a two-tailed paired t-test or Wilcoxon test depending on the normality distribution. The normality distribution was tested with the Shapiro–Wilk test and equal variance was analyzed with Brown–Forsythe test. For intrinsic excitability, a plot of the relation between the number of action potentials and the intensity of the injected current (I–F curve) was created for every neuron in control ACSF and after the drug application. The effect of a drug on excitability was analyzed as the difference in the rheobase, the maximal firing frequency and the difference of the spiking frequency at the same current steps in the comparison to control ACSF.

Data availability

The data and material that support the findings of this study are available upon request to the corresponding author.

Received: 24 March 2023; Accepted: 25 May 2023

Published online: 31 May 2023

References

1. Rudy, B., Fishell, G., Lee, S. & Hjerling-Leffler, J. Three groups of interneurons account for nearly 100% of neocortical GABAergic neurons. *Dev. Neurobiol.* **71**, 45–61 (2011).
2. Wamsley, B. & Fishell, G. Genetic and activity-dependent mechanisms underlying interneuron diversity. *Nat. Rev. Neurosci.* **18**, 299–309 (2017).

3. Kawaguchi, Y. & Kubota, Y. GABAergic cell subtypes and their synaptic connections in rat frontal cortex. *Cereb. Cortex* **7**, 476–486 (1997).
4. Wang, Y. *et al.* Anatomical, physiological and molecular properties of Martinotti cells in the somatosensory cortex of the juvenile rat. *J. Physiol.* **561**, 65–90 (2004).
5. Kvitsiani, D. *et al.* Distinct behavioural and network correlates of two interneuron types in prefrontal cortex. *Nature* **498**, 363–366 (2013).
6. Pi, H.-J. *et al.* Cortical interneurons that specialize in disinhibitory control. *Nature* **503**, 521–524 (2013).
7. Lovett-Barron, M. *et al.* Dendritic inhibition in the hippocampus supports fear learning. *Science* **343**, 857–863 (2014).
8. Gentet, L. J. *et al.* Unique functional properties of somatostatin-expressing GABAergic neurons in mouse barrel cortex. *Nat. Neurosci.* **15**, 607–612 (2012).
9. Muñoz, W., Tremblay, R., Levenstein, D. & Rudy, B. Layer-specific modulation of neocortical dendritic inhibition during active wakefulness. *Science* **355**, 954–959 (2017).
10. Urban-Ciecko, J., Fanselow, E. E. & Barth, A. L. Neocortical somatostatin neurons reversibly silence excitatory transmission via GABAB receptors. *Curr. Biol.* **25**, 722–731 (2015).
11. Bowery, N. G. *et al.* Bicuculline-insensitive GABA receptors on peripheral autonomic nerve terminals. *Eur. J. Pharmacol.* **71**, 53–70 (1981).
12. Connors, B. W., Malenka, R. C. & Silva, L. R. Two inhibitory postsynaptic potentials, and GABA_A and GABA_B receptor-mediated responses in neocortex of rat and cat. *J. Physiol.* **406**, 443–468 (1988).
13. Deisz, R. A. & Prince, D. A. Frequency-dependent depression of inhibition in guinea-pig neocortex in vitro by GABA_B receptor feed-back on GABA release. *J. Physiol.* **412**, 513–541 (1989).
14. Booker, S. A. *et al.* Differential surface density and modulatory effects of presynaptic GABA(B) receptors in hippocampal cholecystokinin and parvalbumin basket cells. *Brain Struct. Funct.* **222**, 3677–3690 (2017).
15. Fanselow, E. E., Richardson, K. A. & Connors, B. W. Selective, state-dependent activation of somatostatin-expressing inhibitory interneurons in mouse neocortex. *J. Neurophysiol.* **100**, 2640–2652 (2008).
16. Somjen, G. G. *Ions in the Brain: Normal Function, Seizures, and Stroke* (Oxford University Press, 2004).
17. Maffei, A., Nelson, S. B. & Turrigiano, G. G. Selective reconfiguration of layer 4 visual cortical circuitry by visual deprivation. *Nat. Neurosci.* **7**, 1353–1359 (2004).
18. Urban-Ciecko, J., Jouhanneau, J.-S., Myal, S. E., Poulet, J. F. A. & Barth, A. L. Precisely timed nicotinic activation drives SST inhibition in neocortical circuits. *Neuron* **97**, 611–625.e5 (2018).
19. Sanchez-Vives, M. V. & McCormick, D. A. Cellular and network mechanisms of rhythmic recurrent activity in neocortex. *Nat. Neurosci.* **3**, 1027–1034 (2000).
20. Guy, J., Möck, M. & Staiger, J. F. Direction selectivity of inhibitory interneurons in mouse barrel cortex differs between interneuron subtypes. *Cell Rep.* **42**, 111936 (2023).
21. Perez-Zabalza, M. *et al.* Modulation of cortical slow oscillatory rhythm by GABA(B) receptors: An in vitro experimental and computational study. *J. Physiol.* **598**, 3439–3457 (2020).
22. Kaplanian, A., Vinos, M. & Skalióra, I. GABA(B) - and GABA(A) -receptor-mediated regulation of Up and Down states across development. *J. Physiol.* **600**, 2401–2427 (2022).
23. Urban-Ciecko, J. & Barth, A. L. Somatostatin-expressing neurons in cortical networks. *Nat. Rev. Neurosci.* **17**, 401–409 (2016).
24. Kapfer, C., Glickfeld, L. L., Atallah, B. V. & Scanziani, M. Supralinear increase of recurrent inhibition during sparse activity in the somatosensory cortex. *Nat. Neurosci.* **10**, 743–753 (2007).
25. Silberberg, G. & Markram, H. Disynaptic inhibition between neocortical pyramidal cells mediated by Martinotti cells. *Neuron* **53**, 735–746 (2007).
26. Pala, A. & Petersen, C. C. H. In vivo measurement of cell-type-specific synaptic connectivity and synaptic transmission in layer 2/3 mouse barrel cortex. *Neuron* **85**, 68–75 (2015).
27. Fino, E. & Yuste, R. Dense inhibitory connectivity in neocortex. *Neuron* **69**, 1188–1203 (2011).
28. Jiang, X. *et al.* Principles of connectivity among morphologically defined cell types in adult neocortex. *Science* **350**, aac9462 (2015).
29. Booker, S. A. *et al.* Presynaptic GABA(B) receptors functionally uncouple somatostatin interneurons from the active hippocampal network. *Elife* **9**, e51156 (2020).
30. Booker, S. A. *et al.* Postsynaptic GABA(B)Rs inhibit L-type calcium channels and abolish long-term potentiation in hippocampal somatostatin interneurons. *Cell Rep.* **22**, 36–43 (2018).
31. Jouhanneau, J.-S., Kremkow, J. & Poulet, J. F. A. Single synaptic inputs drive high-precision action potentials in parvalbumin expressing GABA-ergic cortical neurons in vivo. *Nat. Commun.* **9**, 1540 (2018).
32. Avermann, M., Tómm, C., Mateo, C., Gerstner, W. & Petersen, C. C. H. Microcircuits of excitatory and inhibitory neurons in layer 2/3 of mouse barrel cortex. *J. Neurophysiol.* **107**, 3116–3134 (2012).
33. Lüscher, C., Jan, L. Y., Stoffel, M., Malenka, R. C. & Nicoll, R. A. G protein-coupled inwardly rectifying K⁺ channels (GIRKs) mediate postsynaptic but not presynaptic transmitter actions in hippocampal neurons. *Neuron* **19**, 687–695 (1997).
34. Kaupmann, K. *et al.* GABA(B)-receptor subtypes assemble into functional heteromeric complexes. *Nature* **396**, 683–687 (1998).
35. Degro, C. E., Kulik, A., Booker, S. A. & Vida, I. Compartmental distribution of GABA_B receptor-mediated currents along the somatodendritic axis of hippocampal principal cells. *Front. Synaptic. Neurosci.* **7**, 6 (2015).
36. Sloviter, R. S., Ali-Akbarian, L., Elliott, R. C., Bowery, B. J. & Bowery, N. G. Localization of GABA(B) (R1) receptors in the rat hippocampus by immunocytochemistry and high resolution autoradiography, with specific reference to its localization in identified hippocampal interneuron subpopulations. *Neuropharmacology* **38**, 1707–1721 (1999).
37. Liu, Y., Yang, X. J., Xia, H., Tang, C.-M. & Yang, K. GABA releases from parvalbumin-expressing and unspecific GABAergic neurons onto CA1 pyramidal cells are differentially modulated by presynaptic GABA(B) receptors in mouse hippocampus. *Biochem. Biophys. Res. Commun.* **520**, 449–452 (2019).
38. Shao, C. *et al.* Presynaptic GABA(B) receptors differentially modulate GABA release from cholecystokinin and parvalbumin interneurons onto CA1 pyramidal neurons: A cell type-specific labeling and activating study. *Neurosci. Lett.* **772**, 136448. <https://doi.org/10.1016/j.neulet.2022.136448> (2022).
39. Kruglikov, I. & Rudy, B. Perisomatic GABA release and thalamocortical integration onto neocortical excitatory cells are regulated by neuromodulators. *Neuron* **58**, 911–924 (2008).
40. Takesian, A. E., Kotak, V. C., Sharma, N. & Sanes, D. H. Hearing loss differentially affects thalamic drive to two cortical interneuron subtypes. *J. Neurophysiol.* **110**, 999–1008 (2013).
41. Liguz-Leczner, M., Urban-Ciecko, J. & Kossut, M. Somatostatin and somatostatin-containing neurons in shaping neuronal activity and plasticity. *Front. Neural Circuits* **10**, 48 (2016).
42. Isaacson, J. S. & Scanziani, M. How inhibition shapes cortical activity. *Neuron* **72**, 231–243 (2011).
43. Kuljis, D. A. *et al.* Fluorescence-based quantitative synapse analysis for cell type-specific connectomics. *eNeuro* <https://doi.org/10.1523/ENEURO.0193-19.2019> (2019).
44. Lefort, S. & Petersen, C. C. H. Layer-dependent short-term synaptic plasticity between excitatory neurons in the C2 barrel column of mouse primary somatosensory cortex. *Cereb. Cortex* **27**, 3869–3878 (2017).
45. Kawaguchi, Y. & Shindou, T. Noradrenergic excitation and inhibition of GABAergic cell types in rat frontal cortex. *J. Neurosci.* **18**, 6963–6976 (1998).

46. Kinnischtzke, A. K., Simons, D. J. & Fanselow, E. E. Motor cortex broadly engages excitatory and inhibitory neurons in somatosensory barrel cortex. *Cereb. Cortex* **24**, 2237–2248 (2014).
47. Chen, N., Sugihara, H. & Sur, M. An acetylcholine-activated microcircuit drives temporal dynamics of cortical activity. *Nat. Neurosci.* **18**, 892–902 (2015).
48. Gil, Z., Connors, B. W. & Amitai, Y. Differential regulation of neocortical synapses by neuromodulators and activity. *Neuron* **19**, 679–686 (1997).
49. Davies, C. H., Starkey, S. J., Pozza, M. F. & Collingridge, G. L. GABA autoreceptors regulate the induction of LTP. *Nature* **349**, 609–611 (1991).
50. Mott, D. D. & Lewis, D. V. Facilitation of the induction of long-term potentiation by GABAB receptors. *Science* **252**, 1718–1720 (1991).
51. Wang, L. & Maffei, A. Inhibitory plasticity dictates the sign of plasticity at excitatory synapses. *J. Neurosci.* **34**, 1083–1093 (2014).
52. Kleinjan, M. S. *et al.* Dually innervated dendritic spines develop in the absence of excitatory activity and resist plasticity through tonic inhibitory crosstalk. *Neuron* <https://doi.org/10.1016/j.neuron.2022.11.002> (2022).
53. Finnerty, G. T., Roberts, L. S. & Connors, B. W. Sensory experience modifies the short-term dynamics of neocortical synapses. *Nature* **400**, 367–371 (1999).
54. Steriade, M., Timofeev, I. & Grenier, F. Natural waking and sleep states: A view from inside neocortical neurons. *J. Neurophysiol.* **85**, 1969–1985 (2001).
55. Barth, A. L. & Poulet, J. F. A. Experimental evidence for sparse firing in the neocortex. *Trends Neurosci.* **35**, 345–355 (2012).

Acknowledgements

Special thanks to Joanne Steinmiller for expert animal care, Megumi Matsushita, Rogan Grant and Stephanie E. Myal for technical assistance.

Author contributions

Conceived and designed the work: J.U.C., A.L.B. Acquisition, analysis and interpretation: J.U.C., D.K., K.B. Drafting the manuscript work and revising it critically for important intellectual content: J.U.C., A.L.B., D.K., K.B. All authors have read and approved the final version of this manuscript.

Funding

This work was supported by the National Science Centre, Poland (2015/18/E/NZ4/00721 and 2020/39/B/NZ4/01462 to JUC).

Competing interests

The authors declare no competing interests.

Additional information

Supplementary Information The online version contains supplementary material available at <https://doi.org/10.1038/s41598-023-35890-2>.

Correspondence and requests for materials should be addressed to J.U.-C.

Reprints and permissions information is available at www.nature.com/reprints.

Publisher's note Springer Nature remains neutral with regard to jurisdictional claims in published maps and institutional affiliations.



Open Access This article is licensed under a Creative Commons Attribution 4.0 International License, which permits use, sharing, adaptation, distribution and reproduction in any medium or format, as long as you give appropriate credit to the original author(s) and the source, provide a link to the Creative Commons licence, and indicate if changes were made. The images or other third party material in this article are included in the article's Creative Commons licence, unless indicated otherwise in a credit line to the material. If material is not included in the article's Creative Commons licence and your intended use is not permitted by statutory regulation or exceeds the permitted use, you will need to obtain permission directly from the copyright holder. To view a copy of this licence, visit <http://creativecommons.org/licenses/by/4.0/>.

© The Author(s) 2023